T E C H N I C A L

R E P O R T

0463

FLEXIBLE MODELING OF NEURON FIRING RATES ACROSS DIFFERENT EXPERIMENTAL CONDITIONS. AN APPLICATION TO NEURAL ACTIVITY IN THE PREFRONTAL CORTEX DURING A DISCRIMINATION TASK

CADARSO-SUAREZ, C., ROCA-PARDINAS, J., MOLENBERGHS, G., FAES, C., NACHER, V., OJEDA, S. and C. ACUNA

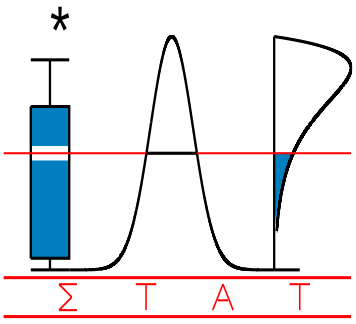

I A P S T A T I S T I C S

N E T W O R K

INTERUNIVERSITY ATTRACTION POLE

http://www.stat.ucl.ac.be/IAP

Flexible modeling of neuron firing rates across different experimental conditions. An application to neural activity in the prefrontal cortex during a discrimination task.

Carmen Cadarso-Suárez[1], Javier Roca-Pardiñas[2], Geert Molenberghs[3], Christel Faes[3], Verónica Nácher[4], Sabiela Ojeda[4], and Carlos Acuña[4]

[1]Department of Statistics and Operations Research, University of Santiago de Compostela, Spain. [*]*email*: eicadar@usc.es

[2]Department of Statistics and Operations Research, University of Vigo, Spain

[3]Center for Statistics, Limburgs Universitair Centrum, Belgium

[4]Department of Physiology, University of Santiago de Compostela, Spain

SUMMARY. In many electrophysiological experiments the main objectives include estimation of the firing rate of a single neuron, as well as a comparison of its temporal evolution across different experimental conditions. To accomplish these two goals, we propose a flexible approach based on the logistic Generalized Additive Model including condition-by-time interactions. We establish that the use of the temporal odds-ratio (OR) curves based on this type of models is very useful in discriminating between the conditions under which the firing probability is higher. Bootstrap techniques are used to construct pointwise confidence bands for the true OR curves. Finally, we apply the new methodology to assessing relationships between neural response and decision making in movement-selective neurons in the prefrontal cortex of behaving monkeys.

KEY WORDS: Extracellular single unit; Firing rates; Behaving monkeys; Generalized additive models; Interaction; Bootstrap.

1. Introduction

One of the techniques used in neurophysiology is electrophysiology, which records the electrical activity produced by neurons. A version of this technique records the activity of single cells in the form of action potentials –or spikes- which typically last about 1 ms. Each time the neuron is excited it produces extracellular action potentials which are transmitted from neuron to neuron. Repeated presentation of the same stimulus provokes a variable number of action potentials. In addition, the time between spikes is very irregular. Although the nature of the neural code is not clear at the present time, the firing or spike rate of neurons and its temporal evolution is considered a measurement of the sensory, motor or behavioral activity. Since the frequency code is the way by which neurons communicate, it is important to the physiologist to assess the neural firing rate.

This electrophysiological technique also allows one to study the correlation between sensory stimuli, or a behavioral act, and the neural response in any part of the brain, such as in the visual or the prefrontal cortices. For example, in the visual cortex, it might be interesting to study the association between oriented lines and the firing rate of the neurons. Lines with different orientation, placed over the receptive field of a visual cell, produce different firing rates.

Our work is motivated by electrophysiological experiments conducted in the prefrontal cortex of behaving monkeys (see Section 2 for a detailed description of this type of experiments). The goal of this study is to determine the possible association between electrical activity of the single neurons and a behavioral act. It is recognized that the prefrontal cortex seems to be critical in the process requiring the use of sensory information to reach a goal (Fuster, 2001). In this context, some prefrontal cortex cells

change their firing rate in advance of an impending movement and some of them are movement selective. Selection of a particular movement depends on a previous decision based on alternatives. This is the case when subjects discriminate the differences in orientation of two bars presented sequentially in front of them, and report the result of the discrimination. The main aim of this electrophysiological study was to find out whether the firing rate of these movement-selective neurons is influenced by decision making.

Formally, data from this type of electrophysiological experiments are collected across time, over a number of trials, and these data are in the form of counts of spikes per unit of time. For an individual neuron, the number of spikes aggregated over the available trials may then be modeled as random variables following a inhomogeneous Poisson counting process with intensity $\lambda(t)$. This function represents the instantaneous mean firing rate for that neuron. Most statistical methods for estimating $\lambda(t)$ are based upon the measurement of the firing times or the inter-spike intervals. The most popular statistical approach (very common in electrophysiological laboratories) is empirical, and consists of averaging spike counts across trials by using the Peri-Stimulous Time Histogram (PSTH) (Gerstein and Kiang, 1960). Such a histogram is obtained by counting the action potentials in consecutive time intervals (bins) of equal width δ (typically of 5 or 10 ms.). This bin width is typically chosen based on the inter-spike intervals.

With the PSTH approach, however, the local firing rate is influenced only by the spikes falling within the time window, rendering the observation of fine temporal changes of the firing activity a difficult task. The problem is further complicated when the mean firing rate is low or the local firing rate fluctuates rapidly. To improve the

estimation of $\lambda(t)$, flexible methods based on smoothing techniques are then advisable (Kass et al., 2003). In the recent literature, two ways to accomplish such smoothing have been explored. Some authors (Szüzcs, 1998; Nawrot, Aersten, and Rotter, 1999) have suggested the use of kernel (firing times) density estimation procedures, while others (DiMatteo, Genovese, and Kass; 2001; Ventura et al., 2002) have proposed modeling spike counts through flexible Poisson regression methods. Although these two methods lead to nearly identical estimates of the firing rate, further advantages of using regression model-based approaches include the possibility of incorporating covariate information to explain differences in the course of the neuronal activity.

The main objective of this paper is to derive a nonparametric regression method for modeling temporal evolution of single-neuron firing rates. In comparison with other existing regression methods, in which spikes are aggregated into bins of width $\delta > 1$ ms., our approach discretizes the data down to bins of 1 ms in width in order no to lose information. In this way, our outcome is binary (spike/no spike) and then it is easy to see that any regression model providing an estimate of the firing probability, also yields an estimate of the firing rate. In this work, we suggest the use of a logistic generalized additive model (GAM) (Hastie and Tibshirani, 1990) which expresses the firing probability as a smooth function of time. The proposed technique does not impose a parametric form on the time effect. Instead, it assumes only that this effect is reasonably smooth, which can be estimated by using a variety of nonparametric local smoothing methods. We will use local linear kernel smoothers.

As mentioned earlier, a main goal in our case study, is to examine possible differences in single-neuron firing rate when the monkey decides whether a test bar (*test* stimulus) is oriented to the left or to the right of another bar shown previously

(*reference* stimulus). To assess the temporal effect of 'orientation' on the firing rate, we will introduce the 'orientation by time' interaction term in the logistic GAM. In this way, the resulting GAM produces different firing profiles for each level of the covariate 'orientation'. To further quantify time periods in which discharges in both orientations are different, i.e. when the cell firing rate discriminates between both decisions, we then compute the temporal odds-ratio (OR) curve for orientation. This curve measures, at each instant, the strength of association between orientation and firing rate.

It should be noticed that our GAM methodology is quite flexible, and extensions to more complex interaction models are straightforward. For instance, we may use the GAM approach to construct factor-by-time interaction models, whereby the factor-by-time terms vary across levels of a categorical variable. Again, this is the case in our example, in which physiologists are interested in examining possible variations in the relationship between neuron response and decision making, when several levels of difficulty in discrimination task are considered.

The article is organized as follows. In Section 2 the electrophysiological experiment is discussed. Logistic GAMs with factor-by-time interactions are introduced in Section 3, and ORs are defined in this context. Section 3.2 describes the estimation method of the logistic GAM with interactions, by using a modified version of the local scoring estimation algorithm combined with local linear kernel smoothers. Cross-validation techniques were also used to determine optimal smoothing parameters in the estimation process. In Section 3.3, we propose bootstrap methods for (i) bias correction in the nonparametric OR estimation; and (ii) construction of confidence intervals for the true ORs. In Section 4, we present the main results obtained for our study, and in

Section 5 we offer some concluding remarks. Some mathematical details were relegated to an appendix.

2. The electrophysiological experiment

The data analyzed here come from studies in our laboratory of the extra-cellular single unit activity in the prefrontal cortex of behaving monkeys. We trained monkeys for several months to discriminate line orientations, in a modified "2 alternative force choice task" (Vázquez, Cano, and Acuña, 2000). A stimulus consisted of a stationary line segment subtending 3º of visual angle. Test lines, 10 per reference, were presented clockwise or counter-clockwise to the reference in steps of 1º. A trial, which lasts about 3 s., was initiated with the presentation of the fixation target at the centre of the monitor screen (Figure 1). Subjects were required to maintain the hand on a lever key through a variable pre-stimulus delay (600-900 ms). Then, two stimuli (called *reference* and *test*), each of 500 ms of duration were presented in temporal sequence, with a fixed inter-stimulus interval (ISI: 1100 ms). At the end of the second stimulus, the subject released the key, in a 1200 ms time window, and pressed one of the two switches (left or right), indicating whether the orientation of the second stimulus was clockwise or counter-clockwise to the first stimulus. Monkeys were rewarded with a drop of water for correct discrimination. While the monkeys worked on the task, we recorded the extra cellular unit activity in the prefrontal cortex.

To get enough data and to account for the cell response variability, the neuron was recorded over a number of $N = 80$ trials. Presentation of the different stimuli is randomly interleaved to avoid cell adaptation to the same stimulus. For each of the $j = 1,\ldots,N$ trials, the following (trial-specific) covariates were considered:

a) Orientation of the *test* stimuli ($Orien^j$): $Orien^j = 0$, if *test* stimulus is to the right of the *reference* stimulus (reference angle is 90º), and $Orien^j = 1$, if *test* stimulus is to the left.

b) Difficulty of the *test* stimuli (Dif^j): Denoting by *TA* the angle corresponding to the *test* stimulus, $Dif^j = 0$ if $TA \in \{78º, 102º\}$ (*test* stimuli more separated from the *reference*, and then very easy to discriminate), $Dif^j = 1$ if $TA \in \{81º, 99º\}$ (*test* stimuli are easy to discriminate), $Dif^j = 2$ if $TA \in \{84º, 96º\}$ (*test* stimuli are difficult to discriminate), and $Dif^j = 3$ if $TA \in \{87º, 93º\}$ (*test* stimuli closest to the *reference*, therefore more difficult to discriminate).

The monkey got the reward in 66 trials. The 14 trials in which the monkey did not get the reward were not used.

In this experiment, the outcome of interest is the neuronal activity. At each instant $t \in [t_{\min}, t_{\max}] = [-500, 4500]$, and trial $j = 1, \ldots, N$, this outcome may be then represented by a temporal binary sequence, Y_t^j, where $Y_t^j = 1$ if there is a spike in $[t, t+1 \text{ ms.})$ and 0 otherwise. Accordingly, for those blocks of *N* trials, the data set consists of the following information: $\left\{ \left(t, Dif^j, Orien^j, Y_t^j \right)_{t=t_{\min}}^{t_{\max}} \right\}_{j=1}^{N}$.

The upper plot of Figure 2 shows the rasters of the response of a neuron recorded in the prefrontal cortex of a monkey while performing in the visual discrimination task, which is described in Figure 1. Each row represents a trial and each tick represents an action potential (spike). The spontaneous cell activity, i.e., in absence of any stimuli, is very irregular, as can be seen in the rasters of Figure 2 (from -500 to 0 ms). Furthermore, during the task performance (from 0 to 2500 ms) the

neural activity is also irregular and changes from trial to trial, something that was noted in other systems from the beginning of this technique (Adrian and Zotterman, 1926). The lower plot of Figure 2 shows the data pooled across trials and then represented through a PSTH of precision $\delta = 10$ ms, and the corresponding kernel smoothed version. Units of mean firing rate are number of spikes per second per trial. As can be seen in this plot, the temporal evolution of the cell firing rate during the task indicates that there is an increase of the firing rate between 1750 ms and 2750 ms, which corresponds to the presentation of the test stimulus and to the reaction time, before the monkey motor response (KU, Figure 2). Therefore, we restricted the data to the time interval between 1500 ms and 3000 ms. One hundred milliseconds before the test stimulus (Figure 2: time scale from 1500 to 1600 ms.) were taken as control because there were no stimuli present and the firing rate variability from trial to trial was very low.

3. Statistical models

In this section, we will define the instantaneous firing rate for a single neuron. Then, we propose the use of various GAMs including interactions, to assess possible associations between neural activity and certain covariates related to decision making.

3.1 Instantaneous Firing Rate

Let $t \in [t_{\min}, t_{\max}]$ be the time period of interest, and let $\{u_i\}_{i=1}^{m}$ denote the point process of spike times aggregated over the *N* trials. For $t \in [t_{\min}, t_{\max}]$, let $N(t)$ be the sample path of the associated counting process. This sample path is a right continuous function that jumps one unit at the spike times and is constant otherwise. In this way, $N(t)$ counts the number and location of spikes in the interval $[t_{\min}, t_{\max}]$. Assuming that

the point process is an inhomogeneous Poisson process (i.e., there is independence between spike times), we define the *firing rate* (or intensity) function as

$$\lambda(t) = \lim_{\Delta t \to 0} \frac{p\left[N(t+\Delta t) - N(t) = 1\right]}{\Delta t} \qquad \text{for } t \in \left[t_{\min}, t_{\max}\right].$$

For sufficiently small intervals $[t, t+\Delta t)$, the average spike count can then be approximated as $\lambda(t)\Delta t$. Furthermore, Δt can be reduced to the point where the probability that more than one spike could appear in this interval is small enough to be ignored. In this case, the average spike occurring during a brief time interval is equal to the value of the instantaneous firing rate during that time interval times the length of the interval.

As we already noted, in our example data were recorded to $\delta = 1$ ms. accuracy. In this way, there is at most one spike in any interval $[t, t+\Delta t)$ and then we may convert the spike times $\{u_i\}_{i=1}^{m}$ into a binary sequence, Y_t , where $Y_t = 1$ if there is a spike in $[t, t+1 \text{ ms.})$ and 0 otherwise. Thus, Y_t is a Bernoulli random variable with probability of spike at $[t, t+1 \text{ ms.})$ defined as $p(Y_t = 1) \simeq \lambda(t)$. This relationship between $\lambda(t)$ and $p(Y_t = 1)$ allows us to approximate the firing rate through any model representing the firing probability as a function of time. Specifically, in Section 3.2., we will propose the use of a logistic GAM. This approach allows for flexible estimation of the single-neuron firing rate as a smooth function of time, with the form of this function depending on several covariates associated with decision making.

3.2 Logistic Generalized Additive Models including Interactions

We use generalised additive modelling to accomplish the following two goals: (i) to examine the temporal association between electrical activity of a single neuron

and decision making; and (ii) to assess whether the association between neural activity and decision making depends on the difficulty of the discrimination task.

First, we consider the following logistic GAM:

$$\log\left(\frac{p(Orien,t)}{1-p(Orien,t)}\right)=\alpha_0+\alpha_1 t+f(t)+g(Orien,t)\ , \tag{3.1}$$

where $p(Orien,t)=p(Y_t=1\,|\,Orien,t)$, α_0 and α_1 are a fixed parameters, $f(t)$ a time function, and g the orientation-by-time interaction term given by

$$g(Orien,t)=g_0(t)\,I_{\{Orien=0\}}+(\beta+g_1(t))\,I_{\{Orien=1\}}\ ,$$

where β is a fixed parameter, and g_0 and g_1, two one-dimensional functions of time. Clearly, the representation given in (3.1) is not unique, and constraints must be placed on $f(t)$ and $g(Orien,t)$. A convenient choice is $E\left[f(t)\right]=0$, $E\left[g(Orien,t)\,|\,Orien\right]=0$, and $E\left[g(Orien,t)\,|\,t\right]=0$.

To assess the temporal association between firing probability (or equivalently, the firing rate) and decisions based on the orientation (1=left; 0=right) of the *test* stimulus, we propose the use of odds-ratios (OR). In accordance with model (3.1), we define $OR(t)$ at each instant t, as

$$OR(t)=\frac{p(1,t)/(1-p(1,t))}{p(0,t)/(1-p(0,t))}=\exp(\beta+g_1(t)-g_0(t)) \tag{3.2}$$

taking the 'right' orientation (i.e., $Orien=0$) as the reference category.

Next to its use as a measure of the effect of orientation on the firing probability, the OR may also be interpreted as a measure of the *discrimination capability* of the neuron.

Since the task difficulty might influence the monkey's behaviour and the neuron firing rate, we are also interested in assessing associations between neuronal activity

and decision making according to the difficulty to discriminate the *test* stimuli, from those very easy to discriminate ($Dif = 0$), to those very difficult to discriminate ($Dif = 3$). Now, denoting $p(Orien, Dif, t) = p(Y_t = 1 | Orien, Dif, t)$, we consider the following GAM:

$$\log\left(\frac{p(Orien, Dif, t)}{1 - p(Orien, Dif, t)}\right) = \alpha_0 + \alpha_1 t + f(t) + g(Orien, Dif, t), \qquad (3.3)$$

with

$$g(Orien, Dif, t) = \beta I_{\{Orien=1\}} + \sum_{l=1}^{3} \gamma_l I_l + \sum_{(k,l)\in \mathbf{A}\setminus(0,0)} \delta_{kl} I_{kl} + \sum_{(k,l)\in \mathbf{A}} g_{kl}(t) I_{kl},$$

where α_0, α_1, β, $\{\gamma_l\}$ and $\{\delta_{kl}\}$ are parameters, $I_l = I_{\{Orien=l\}}$ and $I_{kl} = I_{\{(Orien,Dif)=(k,l)\}}$ are indicator variables, $\{g_{kl}(t)\}$ is a set of one-dimensional functions of time, and $\mathbf{A} = \{(k,l)\ k = 0,1;\ l = 0,1,2,3\}$ is a set of indices.

As in model (3.1), identification of model (3.3) is warranted by assuming $E[f(t)] = 0$, $E[g(Orien, Dif, t) | Orien, Dif] = 0$ and $E[g(Orien, Dif, t) | t] = 0$.

Assuming model (3.3), for each level of difficulty *l*, we may derive the following temporal odds-ratio curves

$$OR_l(t) = \exp\left(\beta + \delta_{1l} - \delta_{0l} + g_{1l}(t) - g_{0l}(t)\right), \qquad (l = 0, \ldots, 3). \qquad (3.4)$$

3.3 Estimation of the GAM including Interactions. The Local Scoring Algorithm

To date, some contributions to GAMs with factor-by-curve interactions like models ((3.1) or (3.3) are found in the literature. Hastie and Tibshirani (1990, p. 265-266) discussed various approaches using smoothing splines. More recently, Coull, Ruppert, and Wand (2001) suggested fitting these models using penalized splines. We propose a new method to nonparametrically estimate the GAMs with factor-by-curve

interactions. The estimation algorithm is based on the local scoring (Hastie and Tibshirani, 1990). Briefly, the local scoring algorithm is analogous to the use of iteratively reweighted least squares (McCullagh and Nelder, 1989) for solving likelihood and nonlinear regression equations. At each iteration, an adjusted dependent variable is formed and a regression model is fitted by applying local linear kernel smoothers (Kauermann and Opsomer, 2003) to the adjusted response (See Appendices A and B for details).

Smoothing windows.

One particular concern in fitting GAMs is the selection of reasonable values for local scoring context means that nowadays optimal selection is still a challenging open problem.

Although one could select such parameters in a subjective manner, in this paper we considered two possibilities in this study: the first consists of using the cross-validation technique to choose the windows h, $\{h_{kl}\}$, used in the estimates $\hat{f}$ and $\{\hat{g}_{kl}\}$ ($k = 0,1$; $l = 0,1,2,3$) (see Appendix A below). The other possibility consists of using the "half-sampling" method. Specifically, the database was split into two sub-samples, in such a way that the first of these (composed of 50% of the data) was used for estimation, and the second for an evaluation of the prediction deviance.

The computational burden involved in window optimization can be handled satisfactorily using binning-type acceleration techniques (Fan and Marron, 1994). Appendix B provides a detailed outline of this procedure when estimating a model like (3.3). The algorithm for estimating model (3.1) is completely analogous, and therefore omitted.

3.4 Nonparametric Estimation of the Odds-Ratio Curves

In this section we focus on the estimation of the temporal OR curves (3.4). The procedure for estimating the OR in (3.2) is completely analogous.

Upon convergence of the algorithm, the resulting estimates of β , $\{\delta_{kl}\}$, and $\{g_{kl}(t)\}$ are inserted in (3.4) to obtain:

$$\widehat{OR}_l(t) = \exp\left(\hat{\beta} + \hat{\delta}_{1l} - \hat{\delta}_{0l} + \hat{g}_{1l}(t) - \hat{g}_{0l}(t)\right), \qquad (l = 0,...,3).$$

At each level of difficulty, *l*, we decide that there exists a significant association between neuronal activity and orientation at instant t, if the corresponding 95 percent confidence interval (CI95%) for the true $OR_l(t)$ does not contain the value one.

To draw inferences about $OR_l(t)$, in this paper we use the binary bootstrap technique suggested by Rodríguez-Campos, González-Manteiga, and Cao (1998). Advantages of these resampling techniques include bias-correction of the estimate $\widehat{OR}(t)$, and also the construction of valid confidence intervals for the true $OR(t)$. Briefly, the proposed mechanism consists of the following steps:

Step 1. Fit model (3), and obtain pilot estimates $\tilde{p}_t^j = \tilde{p}\left(Orien^j, Dif^j, t\right)$ ($t = t_{\min},\ldots,t_{\max}$; $j = 1,\ldots,N$) and then $\widetilde{OR}_l(t)$.

Step 2. For $b = 1,\ldots,B$, generate a sample $\left\{\left(t, Dif^j, Orien^j, Y_t^{j(*b)}\right)_{t=t_{\min}}^{t_{\max}}\right\}_{j=1}^{N}$, where the bootstrap response variable $Y_t^{j,(*b)}$ is distributed in accordance with $Y_t^{j,(*b)} \sim Bernoulli\left(\tilde{p}_t^j\right)$, and calculate the bootstrap estimates $\widehat{OR}_l^{(*b)}(t)$.

Upon completion, the "bootstrap-corrected" odds-ratio estimate at instant t is given by:

$$\widehat{OR}_l(t) - \left(1/B \sum_{b=1}^{B} \widehat{OR}_l^{(*b)}(t) - \widetilde{OR}_l(t)\right).$$

Finally, the $100\% \times (1-\alpha)$ limits for the confidence interval of $OR_l(t)$ are given by $\left(2 \cdot \widehat{OR}_l(t) - a_l^{1-\alpha/2}(t), 2 \cdot \widehat{OR}_l(t) - a_l^{\alpha/2}(t)\right)$ where $a_l^p(t)$ represents the percentile p of the bootstrap estimates $\widehat{OR}_l^{(*1)}(t), \ldots, \widehat{OR}_l^{(*B)}(t)$.

4. Results

As a first step of the analysis we consider the situation in which the monkey takes a decision about the orientation of a bar and signals the result of his decision by moving his hand toward the left or right buttons. All test orientations, clockwise and counter-clockwise to the reference stimulus, which make the monkey take decisions to press the right and left buttons respectively, are then considered. We then fit logistic GAM (3.1) to analyze the difference in firing rate, and its temporal evolution, when the monkey decides. The resulting fit is presented in Figure 4 (left column). In this plot, units for firing rate are number of spikes per second per trial. As can be seen in this figure, for decisions taken to the left, the firing rate is higher than that corresponding to decisions taken to the right. For both decisions, the increase of firing rate begins during the presentation of the test stimulus, and reaches its maximum close to the reaction time (RT), just before the beginning of the arm movement towards the buttons.

To determine the epoch(s) in which the discharge in both situations is different, i.e., when the cell firing rate discriminates between both decisions, we compute the temporal OR curve given in (3.2), taking the 'right' orientation as the reference. In the right plot of Figure 4, we present the resulting OR curve (on a logarithmic scale), along

with the corresponding pointwise 95% bootstrap confidence bands. It is seen that the magnitude of the OR relating orientation to neural response becomes significantly greater than one, 77 ms after the beginning of the presentation of the test stimulus, reaches its maximum around the reaction time and then decreases, losing significance at 2959 ms, when the monkey finishes its arm movement. Therefore, a significant strength of association between firing rate and decisions –which might be interpreted as the *discrimination capability* of the neuron-, is maintained for 1282 ms.

<Put Figure 4 about here>

Decision making depends on the difficulty of the task; the greater the difficulty the longer the reaction time. Because test orientations closer to the reference are more difficult to discriminate than those orientations more apart, reaction times are longer in the first case than in the second. To study the effect the difficulty of discrimination might have on cell responses, we fit the logistic-GAM given in (3.3) to the cell discharges produced during discrimination of orientations. The resulting curves for each difficulty (classified as: very easy, easy, difficult, and very difficult to discriminate), are presented in the left panel of Figure 5. From these plots, it is apparent that the firing rate and temporal evolution of the cell discharge differ when the decisions are to be taken to the left or to the right; the mean firing rate is higher for the very difficult discriminations (67 spikes/s) than for the very easy ones (49 spikes/s). The peak of neural activity associated with the decisions to be taken to the left delays from 2357 ms (time base readings) for the very easy discriminations to 2500 ms for the very difficult ones. The opposite occurs for the peak of neural activity associated with decisions to be taken to the right; in this case the peak for the very easy discriminations (2642 ms) is ahead of the very difficulty ones (2214 ms).

To quantify, moment by moment, the difference of the discharge rate and to assess the discrimination capability of the cell in both situations, we compute the temporal ORs in (3.4), from the fitted GAM (3.3). The resulting curves (on a logarithmic scale), along with their 95% confidence bands, are shown in the right column of Figure 5. For the four levels of difficulty considered, the corresponding firing rates (Figure 5 left column) associated with a monkey's decision to the left, is higher than a neural response associated with a decision to the right. The ORs indicate that the moment at which the neural response begins to discriminate between both situations, i.e., reaches significance, occurs later for the most difficult discriminations (490 ms after the beginning of the test stimulus) than for the easier ones (288 ms after the beginning of the test stimulus). Moreover, the ORs show that the strength of the association given by the deviation from $Log(OR) = 0$ is 33% higher for the very difficult discriminations than for the very easy ones. These neural data correlate well with the behavior of the monkey; it takes more time for monkeys to reach a behavioral decision during the most difficult discriminations than during the easiest ones.

<Put Figure 5 about here>

The results presented in this section were generated using the smoothing windows obtained by the "half-sampling" method. Similar results (not shown here) were achieved using the cross-validation method.

Validity of the Inhomogeneous Poisson (IP) assumption.

So far, we have assumed that the data within trials, and then pooled across trials, follow an IP process. Although limit theory makes this plausible, we like to formally check formally this assumption. To this aim, we use a goodness-of-fit test recently

suggested by Brown et al. (2002). This method is the Quantile-Quantile (Q-Q) plot-based test, which relies on the time-rescaling theorem (Daley and Vere-Jones, 1980). Briefly, this result establishes that if the IP process is correct, then the series of spikes on the transformed scale, $\Lambda(u) = \int_0^u \lambda(t)\,dt$, is a Poisson process of constant unit rate. Hence, if $0 < u_1 < \ldots < u_m$ are the spike times, the rescaled times $z_i = 1 - \exp\left(\Lambda(u_{i-1}) - \Lambda(u_i)\right)$ are independent uniform random variables on the interval (0,1).To check the IP assumption we proceed as follows. First we order the values z_i, denoting the order statistics by $z_{(i)}$. We then plot the values of the cumulative distribution function (CDF) of the uniform variable on (0,1), against the $z_{(i)}$ values. If the IP assumption is correct, then the points should lie on a 45-degree line. In order to measure the degree of departure of the plot from the 45-degree line relative to chance, 95% pointwise confidence bands were constructed, by finding the 2.5th and the 97.5th percentiles of the CDF of each $z_{(i)}$, which follows a $Beta(i, m-i+1)$ distribution (Johnson and Kotz, 1979).

We then estimate the firing rate via kernel smoothing, first globally (i.e., taking all trials together), and then separately, by selecting subsets of trials marked by the different levels of orientation and difficulty. The resulting Q-Q plots are presented in Figure 3.

<Put Figure 3 about here>

As can be seen from this figure, all the Q-Q plots lie within the 95% pointwise confidence bands, indicating that deviations of the IP assumption are not statistically significant. It should be noted that this assumption seems to remain valid even in the

presence of small departures, which occur mainly when the number of trials is small. All of these results lead us to conclude that this IP assumption is satisfactory, and therefore statistical approaches used in this paper are judged as adequate to model the electrical activity of the neuron studied.

5. Discussion

In this paper, a logistic GAM including factor-by-time interactions was proposed as a flexible tool for estimating the time-varying firing rate of a single neuron, which in turn may vary across different experimental conditions. For the statistical comparison of the temporal evolution of this firing rate across different conditions, temporal odds-ratio curves were then constructed, and related inference was carried out through their corresponding bootstrap pointwise confidence bands.

The new methodology was applied to assess whether movement-selective neurons in the prefrontal cortex are influenced by decision making. The application of the logistic GAM showed that the greater the difficulty of the discrimination, the longer the reaction time, and the higher the neural firing rate associated to the discrimination. In this work, we have also shown the usefulness of temporal OR curves based on GAM to discriminate between firing rates of a neuron in an experimental situation in which several covariates are involved in decision making. In our example, the concept of temporal Odds Ratio allowed us to determine the starting point and duration of a neural response associated with monkey decision. We also found that, for these cells, starting point, duration and strength of association of neural discharge with decision making, vary accordingly with the difficulty of the discrimination.

Nonparametric estimation of the GAM including condition-by-time interactions was carried out through a new version of the local scoring algorithm combined with

local linear kernel smoothers. For the automatic choice of bandwidths, we have used cross-validation techniques and half-sampling method. It is well known that automatic choice of bandwidths implies a high computational burden. In our particular database, this burden increases even further, since the sample size is large. For these computational reasons, binning-type acceleration techniques (Fan and Marron, 1994) were used to satisfaction.

Although this work focused mainly on GAMs with only one continuous covariate (i.e., the *time*), extensions of our methodology to the multidimensional case including a set of continuous covariates, are possible. One possibility is to incorporate backfitting techniques into our local smoothing estimation method (which is not needed in the one-covariate case). Alternatively, models used in this paper can be thought as *varying-coefficients* regression models (Hastie and Tibshirani, 1993). Then, one could also apply a number of approaches currently available for estimating this type of models (e.g., Kauermann and Tutz, 1999; Cai, Fan and Li, 2000). Although it is out of the scope of this paper, it could be worthwhile to further explore the behavior of the resulting estimators when applying these alternatives to modelize physiological data. This is a topic for future research.

It is necessary to highlight that the bootstrap pointwise confidence bands for the temporal odds-ratio, represent the 100 percent x (1-α) confidence intervals of the true OR at each of the times along the study period, but they do not allow us to make global inferences about the true OR curves. However, for the neuron studied here, the resulting OR curves give us a quite reasonable representation of the temporal course for the strength of association between firing rates and variables involved in decision making.

In our setting, data pooled across trials were assumed to follow an inhomogeneous Poisson process with instantaneous firing rate $\lambda(t)$. This assumption seems to be justifiable for the studied neuron, according to results obtained from applying the Q-Q plot-based test suggested by Brown, Barbieri et al. (2002). In some instances, however, there is substantial evidence that cortical neurons in behaving animals may have non-Poisson spike times within trials (Barbieri et al., 2001; Kass and Ventura, 2001). The firing probability depends not only on instant t, but also on the history of the process $\mathbf{H}_t$ up to t (Brown et al, 2001). The method described in this paper can easily be adapted to those situations by considering $\mathbf{H}_t = \Delta_t$, Δ_t being the elapsed time between the occurrence of the last spike up to t. In this way, we may use a model like (3.3) including a bidimensional function, $f(t, \Delta_t)$, resulting in a more general model of the form:

$$\text{logit}\left(p\left(Orien, Dif, t, \Delta_t\right)\right) = \left(\beta_0 + f\left(t, \Delta_t\right) + g\left(Orien, Dif, t\right)\right).$$

Finally, it should be emphasized that the GAM-based OR is a measure of general utility for experimental physiology when, for example, a measurement is required to compare neuronal firing rates across several experimental conditions, without assuming a parametric model for the discharge firing rate. With our procedure, GAM allows us at first to incorporate these conditions as (trial-specific) covariates, and later the GAM-based ORs serve us to objectively identify, moment by moment, those conditions in which the firing is higher. In this way, the methodological approach proposed here is, from a practical viewpoint, a fast and reliable analysis tool designed to be used on-line or off-line in the laboratory. It allows assessment of neural activity and its relation to a variety of experimental events.

A FORTRAN program implementing the nonparametric model estimation (with binning) and the OR curves with corresponding confidence bands, can be obtained by contacting second author at roca@uvigo.es.

ACKNOWLEDGEMENTS

This work was partially supported by the Spanish Ministry of Science and Technology (BMF2002-03213, European FEDER support included) to Carmen Cadarso-Suárez; by the University of Vigo (Vigo, Spain) to Javier Roca-Pardiñas, and by the Spanish Ministry of Science and Technology (PM99-0025 and 2003/PC014) to Carlos Acuña. Verónica Nácher and Sabiela Ojeda have fellowships from Spanish Ministry of Science and Technology. The research of Geert Molenberghs was supported by FWO-Vlaanderen Research Project "Sensitivity Analysis for Incomplete and Coarse Data" and Belgian IUAP/PAI network "Statistical Techniques and Modeling for Complex Substantive Questions with Complex Data". The research of Christel Faes was supported by IWT-Vlaanderen.

REFERENCES

Adrian, E.D. and Zotterman, Y. (1926). The impulses produced by sensory nerve-endings. Part 2. The responses of a single end-organ. *Journal of Physiology* (London) **61**, 151-171.

Barbieri, R., Quirk, M.C., Frank, L.M., Wilson, M.A., and Brown E.N. (2001). Construction and analysis of non-Poisson stimulus-response models of neural spike train activity. *Journal of Neuroscience Methods* **105**, 25-37.

Brown, E.N., Barbieri, R., Ventura, V., Kass, R.E., and Frank, L.M. (2002). The time-rescaling theorem and its application to neural spike train data analysis. *Neural Computation* **14**, 325-346.

Cai, Z., Fan, J., and Li R. (2000). Efficient estimation and inferences for varying-coe.cient models. *Journal of the American Statistical Association* **95** (451), 888–902.

Coull, B., Ruppert, D., and Wand, M. (2001). Simple incorporation of interactions into additive models. *Biometrics* **57**, 539-545.

Daley, D.J. and Vere-Jones, D. (1988). *An introduction to the theory of stochastic processes.* New York: Springer Verlag.

DiMatteo, I., Genovese, C.R., and Kass, R.E. (2001). Bayesian curve-fitting with free-knot splines. *Biometrika* **88**, 1055-1071.

Fan, J. and Marron, J.S.(1994). Fast implementation of nonparametric curve estimators. *Journal of Computational and Graphical Statistics* **3**, 35-56.

Fuster, J.M. (2001). The prefrontal cortex-an update: time is of the essence. *Neuron* **30**, 319-333.

Gerstein, G.L. and Kiang, N.Y.S. (1960). An approach to the quantitative analysis of electrophysiological data from single neurons. *Biophysical Journal* **54**, 1513-1528.

Hastie, T.J. and Tibshirani, R.J. (1990). *Generalized Additive Models*. London: Chapman and Hall.

Hastie, T.J. and Tibshirani, R.J. (1993). Varying-coefficient models. *Journal of the Royal Statistical Society* B **55**, 757–796.

Johnson, N.L. and Kotz, S. (1970). *Distributions in statistics: Continuous univariate distributions-2*. New York: Wiley.

Kass, R.E. and Ventura, V. (2001). A spike train probability model. *Neural Computation* **13**, 1713-20.

Kass, R.E., Ventura, V., and Cai, C. (2003). Statistical smoothing of neuronal data. *Network* **14**, 5-15.

McCullagh, P. and Nelder, J.A.(1989). *Generalized Linear Models*. London: Chapman and Hall.

Nawrot, M., Aertsen, A., and Rotter, S. (1999). Single-trial estimation of neuronal firing rates: from single-neuron spike trains to population activity. *Journal of Neuroscience Methods* **94**, 81-92.

Kauermann G. and Opsomer J.D. (2003). Local Likelihood Estimation in Generalized Additive Models. *Scandinavian Journal of Statistics*, **30**, 317-337.

Kauermann, G. and Tutz, G. (1999). On model diagnostics and bootstrapping in varying coefficient models. *Biometrika* **86**, 119-128.

Rodríguez-Campos, M.C., González-Manteiga, W., and Cao, R. (1998). Testing the hypothesis of a generalized linear regression model using nonparametric regression estimation. *Journal of Statistical Planning and Inference* **67**, 99-122.

Szücs, A. (1998). Applications of the spike density function in analysis of neuronal firing patterns. *Journal of Neuroscience Methods* **81**, 159-167.

Vázquez, P., Cano, M., and Acuña, C. (2000). Discrimination of line orientation in humans and monkeys. *Journal of Neurophysiology* **83**, 2639-2648.

Ventura, V., Carta, R., Kass, R.E., Gettner, S.N., and Olson, C.R. (2002). Statistical analysis of temporal evolution in single-neuron firing rates. *Biostatistics* **1**, 1-20.

APPENDIX A

Weighted Local Linear Kernel Estimators

Given a sample $\{t_i, Y_i\}_{i=1}^n$ and a set of weights, $\{W_i\}_{i=1}^n$, the weighted local linear kernel estimator $\hat{\psi}(t) = \hat{\psi}\left(t, \{t_i, Y_i, W_i\}_{i=1}^n, h\right)$ at a localization *t* is defined as:

$$\hat{\psi}(t) = \begin{pmatrix} 1 & 0 \end{pmatrix} \begin{pmatrix} s^0(t) & s^1(t) \\ s^1(t) & s^2(t) \end{pmatrix}^{-1} \begin{pmatrix} u^0(t) \\ u^1(t) \end{pmatrix},$$

where $s(t) = \sum_{i=1}^n \left(W_i \cdot L^r\left(t, t_i\right)\right)$ and $u(t) = \sum_{i=1}^n \left(W_i \cdot L^r\left(x, t_i\right) \cdot Y_i\right)$, with

$$L^r\left(x, y\right) = \frac{\left(x-y\right)^r}{\sqrt{2\pi}} \exp\left(-\frac{1}{2}\left(\frac{x-y}{h}\right)^2\right), \ (r = 0, 1, 2).$$

The smoothing bandwidth, h, can be selected automatically by minimizing the following weighted cross-validation error criterion $CV = n^{-1}\sum_{i=1}^n W_i\left(\hat{\psi}^{-i)}\left(t_i\right) - Y_i\right)^2$, where $\hat{\psi}^{-i)}\left(t_i\right)$ indicates the fit at t_i leaving out the *i*th data point.

APPENDIX B

Estimating a GAM with Factor-by-Time Interactions. Local Scoring Algorithm

The local scoring algorithm for estimating a logistic GAM with interactions given in (3) has the following steps:

Initialization. Compute the initial estimates $\hat{\alpha}_0 = \log\left(\overline{Y}/(1-\overline{Y})\right)$, $\hat{\alpha}_1 = 0$, $\hat{\beta}^0 = 0$, $\hat{\gamma}_l^0 = 0$, $\hat{\delta}_{kl}^0 = 0$, $\hat{f}_t^0 = \hat{f}^0(t) = 0$, $\hat{g}_{kl,t}^0 = \hat{g}_{kl}^0\left(t\right) = 0$ and $\hat{g}_t^{j,0} = \hat{g}^0\left(Orien^j, Dif^j, t\right) = 0$, $(t = t_{\min}, \ldots, t_{\max}; j = 1, \ldots, N)$.

Step 1. Form the adjusted dependent variables $\tilde{\mathbf{Y}}$ and the weights W, so that

$$\tilde{Y}_t^j = \hat{\eta}_t^{j,0} + \frac{Y_t^j - \hat{p}_t^{j,0}}{\hat{p}_t^{j,0}\left(1-\hat{p}_t^{j,0}\right)} \quad \text{and} \quad W_t^j = \frac{1}{\hat{p}_t^{j,0}\left(1-\hat{p}_t^{j,0}\right)},$$

where $\hat{\eta}_t^{j,0} = \hat{\alpha}_0 + \hat{\alpha}_1^0 t + \hat{f}_t^0 + \hat{g}_t^{j,0}$ and $\hat{p}_t^{j,0} = \exp\left(\hat{\eta}_t^{j,0}\right) \Big/ \left(1 + \exp\left(\hat{\eta}_t^{j,0}\right)\right)$.

Step 2. Calculate the partial residuals $R_t^j = \overline{\tilde{Y}_t^j} - \hat{f}_t - \sum_{(k,l)\in\mathbf{A}} \hat{g}_{kl,t}^{j,0} I_{kl}^j$, with $I_{kl}^j = I_{\left\{Orien^j = k, Dif^j = l\right\}}$, and obtain estimates $\hat{\alpha}_1$, $\hat{\beta}$, $\left\{\hat{\gamma}_l\right\}$ y $\left\{\hat{\delta}_{kl}\right\}$ by solving a weighted least squares problem for $\mathbf{R}$, with weights W.

Step 3. Compute the local linear polynomial estimator updates (see Appendix A for details),

$$\hat{f}_t = \hat{\psi}\left(t, \left\{\left(\tilde{t}, R_{\tilde{t}}^{\tilde{j}}, W_{\tilde{t}}^{\tilde{j}}\right)_{\tilde{t}=t_{\min}}^{t_{\max}}\right\}_{\tilde{j}=1}^{N}, h\right) \quad , \quad \left(t = t_{\min}, \ldots, t_{\max}\right)$$

being $R_t^j = \tilde{Y}_t^j - \overline{\tilde{Y}_t} - \hat{\alpha}_1 t - \hat{\beta} I_{\left\{Orien^j = 1\right\}} - \sum_{l=1}^{3} \hat{\gamma}_l I_l^j - \sum_{(k,l)\in\mathbf{A}\setminus\{(0,0)\}} \hat{\delta}_{kl} I_{kl}^j$ the partial residuals, $h > 0$ the smoothing bandwidth, and $\hat{\psi}$, the local linear polynomial estimator defined in Appendix A

Step 4. Compute

$$\hat{g}_{kl}^j(t) = \hat{\psi}\left(t, \left\{\left(\tilde{t}, S_{\tilde{t}}^{\tilde{j}}, W_{kl,\tilde{t}}^j\right)_{\tilde{t}=t_{\min}}^{t_{\max}}\right\}_{\tilde{j}=1}^{N}, h_{kl}\right) \qquad \left(k = 0,1 \;;\; l = 0,1,2,3\right)$$

with $S_t^j = R_t^j - \hat{f}_t$, $W_{kl,t}^j = W_t^j I_{kl}^j$, and $\left\{h_{kl}\right\}$ the bandwidths associated with estimation of g_{kl}.

Step 4. This process is repeated, $\hat{\alpha}_1^0$ being replaced by $\hat{\alpha}_1$, $\hat{\beta}^0$ being replaced by $\hat{\beta}$, $\left\{\hat{\gamma}_l^0\right\}$ by $\left\{\hat{\gamma}_l\right\}$, $\left\{\hat{\delta}_{kl}^0\right\}$ by $\left\{\hat{\delta}_{kl}\right\}$, $\hat{f}_t^0$ by $\hat{f}_t$, and $\hat{g}_t^0$ by $\hat{g}_t$, until, for some small threshold ε, $\left|D\left(\hat{\mathbf{p}}^0, \mathbf{S}\right) - D\left(\hat{\mathbf{p}}, \mathbf{S}\right)\right| \Big/ D\left(\hat{\mathbf{p}}^0, \mathbf{S}\right) \le \varepsilon$

with $D\left(\hat{\mathbf{p}}, \mathbf{Y}\right) = -2\sum_{t=t_0}^{t_J} \sum_{j=1}^{N} \left(Y_t^j \log\left(\hat{p}_t^j\right) + \left(1 - Y_t^j\right) \log\left(1 - \hat{p}_t^j\right)\right)$, being

$\hat{p}_t^{j,0} = \exp\left(\hat{\eta}_t^{j,0}\right) \Big/ \left(1 + \exp\left(\hat{\eta}_t^{j,0}\right)\right)$ and $\hat{\eta}_t^j = \hat{\alpha}_0 + \hat{\alpha}_1 t + \hat{f}_t + \hat{g}_t^j$.

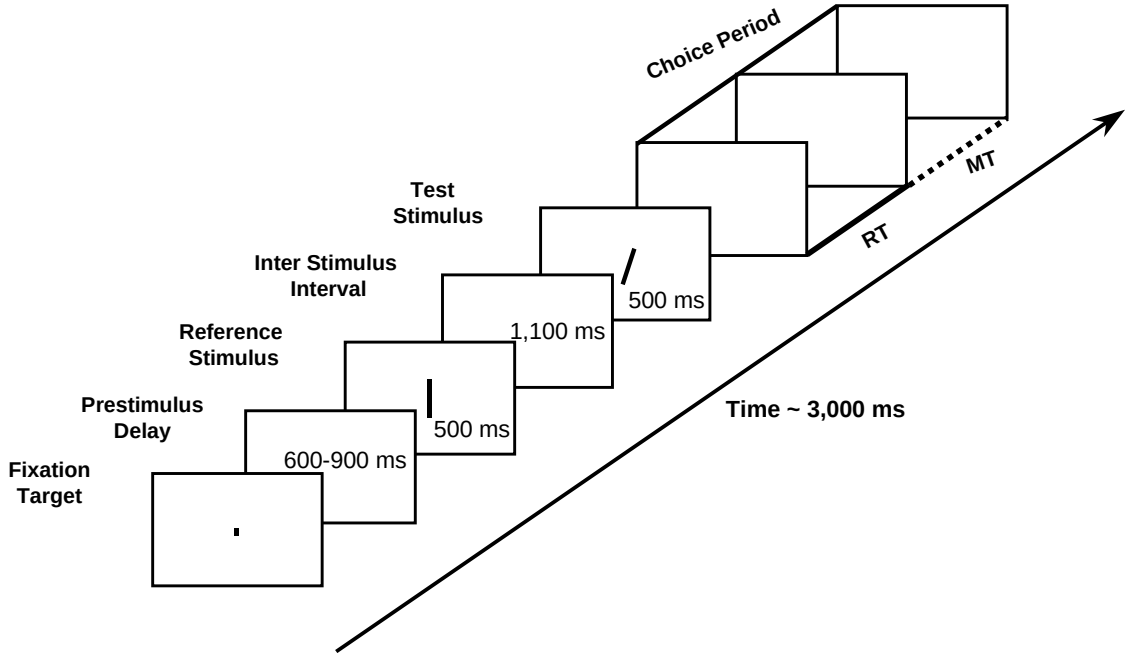

Figure 1. Schematic outline of the orientation discrimination task, described in the text. Neuron was recorded about 80 times. RT: reaction time. MT: movement time.

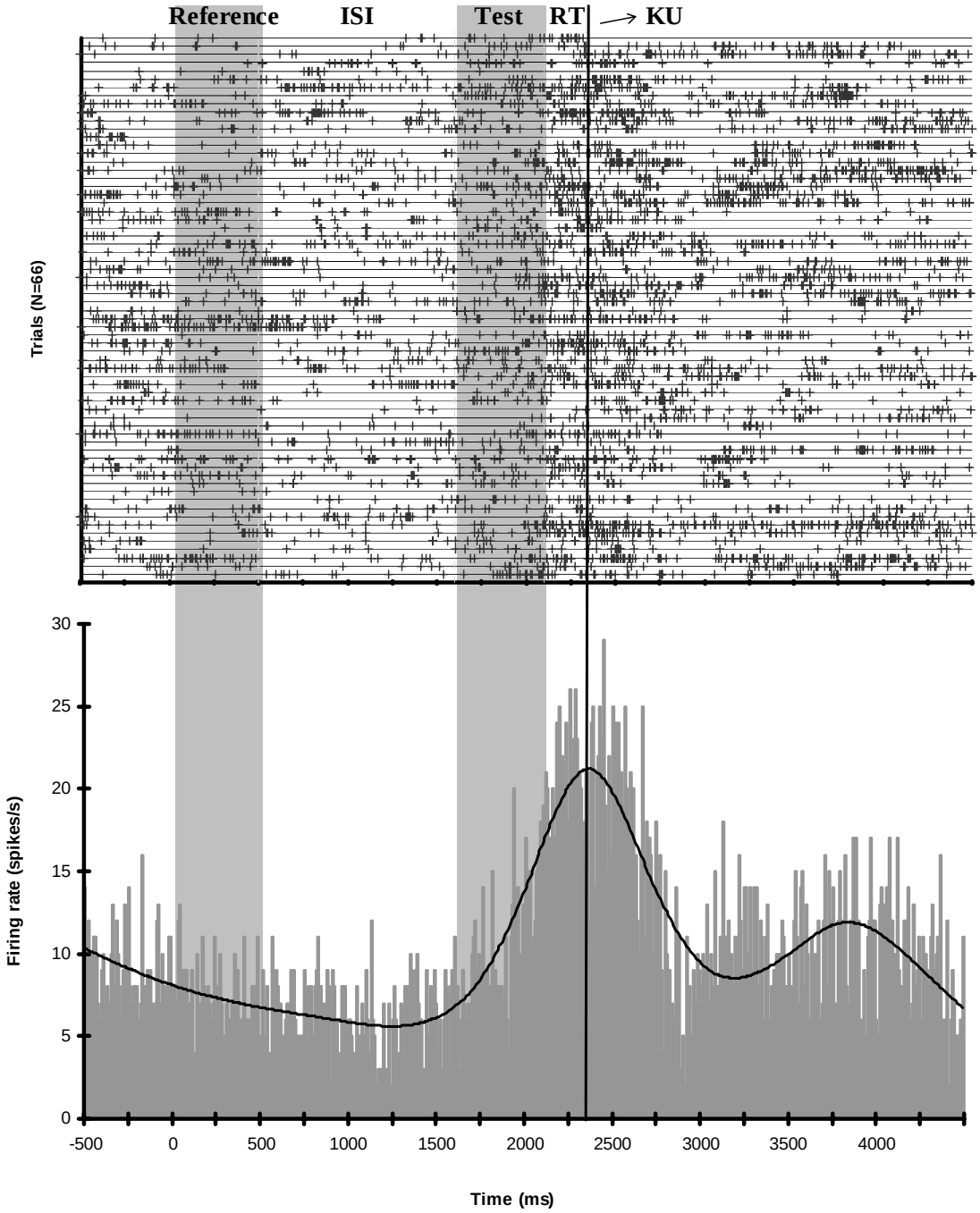

Figure 2. Response of a neuron during the performance of the discrimination task. The raster plot (top panel) shows the observed spikes for each of the 66 trials on separate horizontal lines. The boxes mark task events: presentation of the reference stimulus (from 0 to 500 ms); the interstimulus interval (ISI: 500, 1600ms); the test stimuli (1600 to 2100 ms); the beginning of the motor response (KU: Key Up at 2384 ms). The lower panel shows the observed spikes pooled across trials, displayed as count of spikes occurring within 10 ms. intervals (i.e. the Peristimulus Time Histogram, PSTH), and its kernel smoothed version.

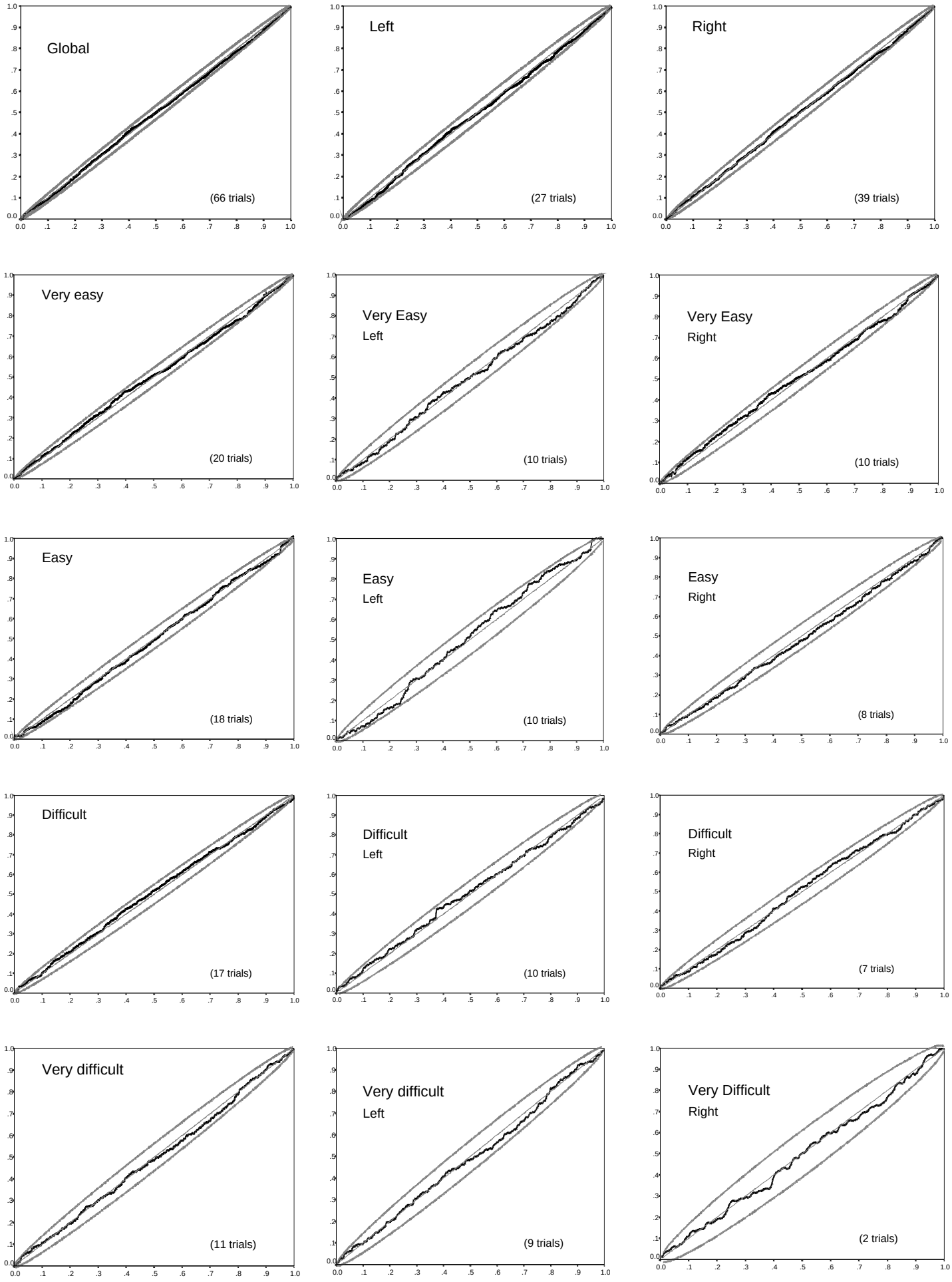

Figure 3. Quantile-Quantile (Q-Q)-based plots of the IP with the corresponding 95% confidence bands.

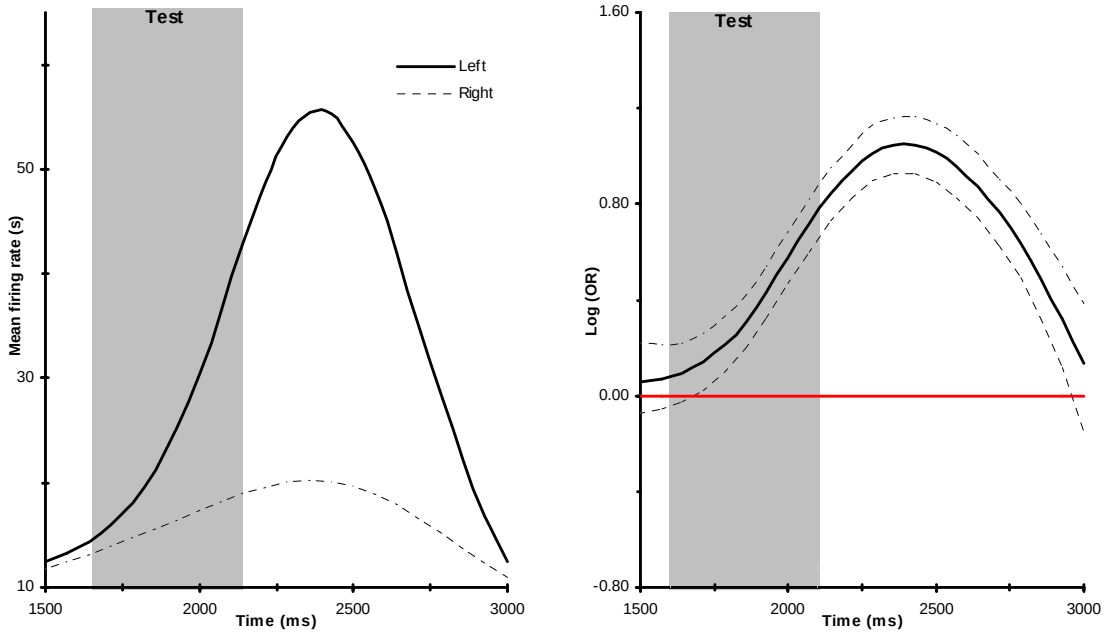

Figure 4. Left plot: Estimated firing rates grouped by orientation (left, right). Right plot: *log (OR)* curve for the association between firing rate and orientation together with the corresponding pointwise 95% confidence bands. Reference orientation: “Right”. Grey boxes indicate the timing of the test stimulus.

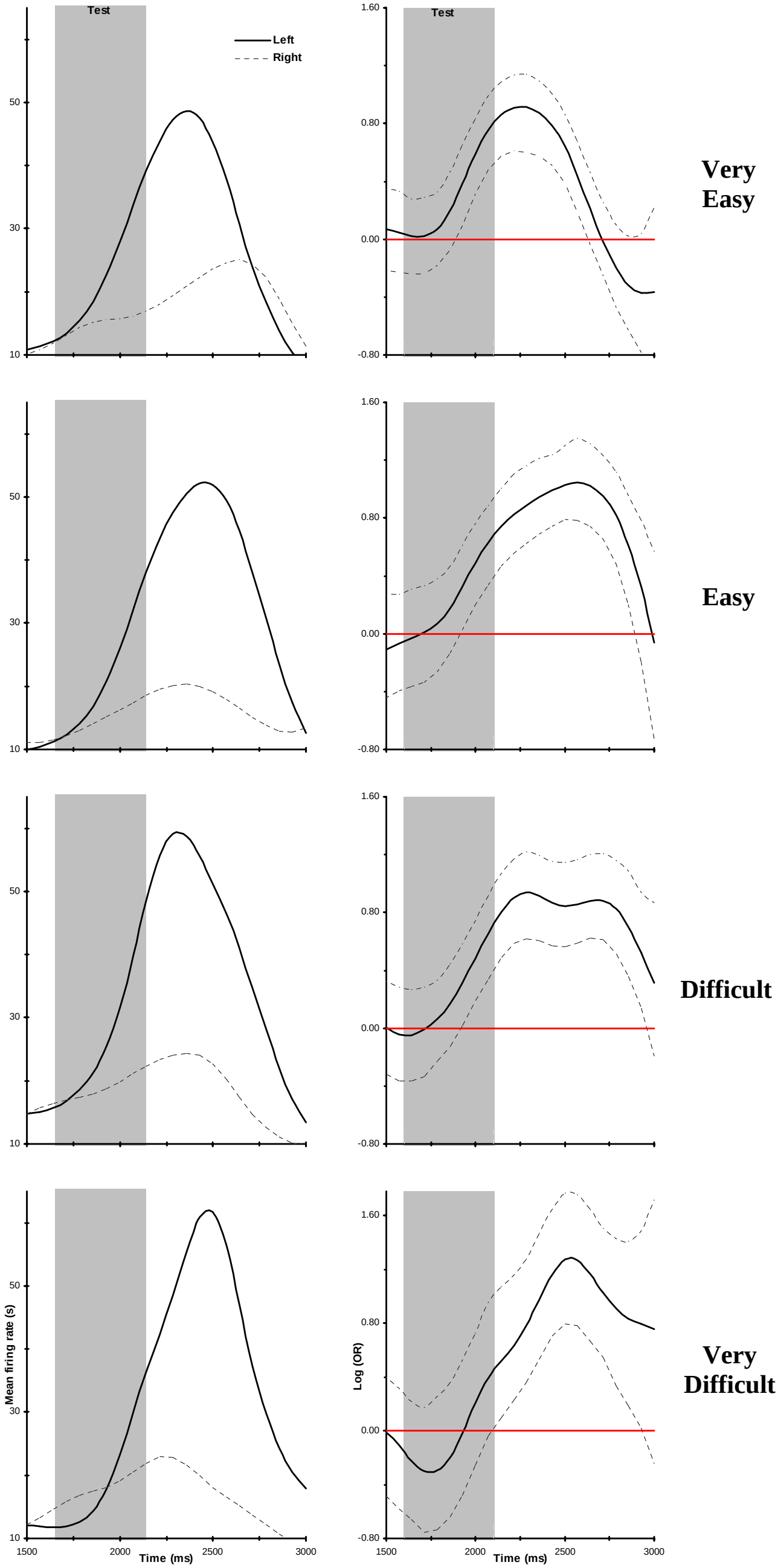

Figure 5. Left panel: Estimated firing rates grouped by orientation (left, right), according to the difficulty of the discrimination. Right panel: *log (OR)* curves for the association between firing rate and orientation together with the corresponding pointwise 95% confidence bands. Reference orientation: “Right”. Grey boxes indicate the timing of the test stimulus.